Journal of Atmospheric and Solar–Terrestrial Physics 199 (2019) 105207

Contents lists available at ScienceDirect

Journal of Atmospheric and Solar-Terrestrial Physics

journal homepage: www.elsevier.com/locate/jastp

Assessment of new thermospheric mass density model using NRLMSISE-00 model, GRACE, Swarm-C, and APOD observations

Andres Calabia, Geshi Tang *, Shuanggen Jin **

School of Remote Sensing and Geomatics Engineering, Nanjing University of Information Science and Technology, Nanjing, 210044, China

ARTICLE INFO

Keywords:
Thermospheric mass density
GRACE
Swarm
APOD
NRLMSISE-00

ABSTRACT

Thermospheric mass density estimates from in-situ observations along satellite orbits are difficult to validate due to their inherent spatiotemporal sparse nature, and difficulties related to drag-force modeling and estimation of actual mass density state. Current upper atmospheric models are unable to accurately represent the actual thermospheric variability, and in-situ observations are far to fulfill the minimum requirements in practical applications. In this manuscript, the new Thermospheric Mass Density Model (TMDM) is based on the fit of solar flux, annual, Local Solar Time (LST), and magnetospheric proxies into the Principal Component Analysis (PCA) of 13 years of accelerometer-based mass density estimates derived from the GRACE (Gravity Recovery and Climate Experiment) mission. We employ the NRLMSISE-00 model and estimates from APOD (Atmospheric density detection and Precise Orbit Determination), Swarm-C, and GRACE satellites, and assess the new model, including statistical analyses, and a Precise Orbit Determination (POD) scheme. We compare 2 years of APOD and Swarm-C estimates, and study the dynamic orbit propagation of the 3 missions under different mass density input schemes and different magnetospheric activity conditions. The results with TMDM show similar differences in the dynamically propagated orbits from NRLMSISE-00 and in-situ observations. The statistical analyses show that NRLMSISE-00 overestimates about 20%, and TMDM underestimates about 20%, the in-situ observations.

1. Introduction

Aerodynamic drag variations at Low Earth Orbit (LEO) are associated with thermospheric mass density fluctuations resulting from the upper atmosphere expansion/contraction in response to variable solar activity. Increased drag decelerates LEO moving the orbits closer to Earth, shortens space-assets lifetime, and makes the tracking of objects difficult. In addition, the exponential increase of space debris (including the recent destructive events of Fengyun-1C, Iridium, and Mission Shakti) has recently highlighted the importance of orbital tracking, and the prediction and avoidance of potential collisions of orbiting satellites have become an essential task. Among these concerns, other negative repercussions could include the damaging effects on satellites and international space stations or the uncontrolled decay and re-entry of space objects with unsafe collisions on Earth.

During the last decades, the scientific community has been motivated to better understand and model the global mass density distribution and variations in the upper atmosphere. This effort aims to better predict LEO trajectories under variable drag conditions (Emmert, (2015)). (Anderson et al., (2009)) showed that not only the rough knowledge of mass density variations acting on the surface of the orbiting objects but also the minor contributions (e.g., wavelengths below the order of 8000 km) can influence LEO trajectories. (Leonard et al., (2012)) showed that in-track prediction differences incurred by tidal mass density effects are typically about 100–300 m for satellites in 400 Km circular orbits at 24 h prediction, exceeding significantly the error magnitudes for US Air Force applications (Anderson et al., 2009). All these aspects indicate the need to improve the current mass density models with more accurate modeling and assimilative techniques to better reproduce and forecast the actual variations.

Nowadays, the rapid development of micro-electro-mechanical systems and satellite technologies which includes accurate tri-axial accelerometers, miniaturized atmosphere detection devices, and precise GNSS receivers, has offered a great new opportunity to detect thermospheric mass density in a more extensive spatiotemporal coverage, and with a relatively very low cost. However, the spatiotemporal sparse nature of observations brings an important limitation for the validation of estimates, due to the inherent orbital configurations of the LEO

* Corresponding author.
** Corresponding author.
E-mail addresses: andres@calabia.com (A. Calabia), tanggeshi@nuist.edu.cn (G. Tang), sgjin@nuist.edu.cn (S. Jin).

https://doi.org/10.1016/j.jastp.2020.105207
Received 13 June 2019; Received in revised form 30 August 2019; Accepted 20 January 2020
Available online 1 February 2020
1364-6826/

satellite missions, which usually do not overlap nor take measurements at the same locations and times (e.g., Figs. 1 and 2). Typically, the validation of observations is performed using most recent empirical models, employing their global capability for prediction in estimating the upper atmosphere state along any possible orbital path. Unfortunately, currently available models of the upper atmosphere are incapable to predict the variability as required, in spite of the efforts to model variations, anomalies, and climatology over the last half-century. This is largely due to the limited quality and quantity of observations used to better characterize the driver-response relationship of variability, and the lack of comprehensive approaches for calibrating the models.

This work aims to prove the predictive capability of the new TMDM to estimate the thermospheric mass density variability. The model is based on parameterizations of solar flux, annual, LST, and magnetospheric proxies into the PCA of 13 years of accelerometer-based mass density estimates derived from the GRACE (Gravity Recovery and Climate Experiment) mission. We compare the new TMDM model to independent measurements made by the APOD (Atmospheric density detection and Precise Orbit Determination), the GRACE, and the Swarm missions. Moreover, we include the NRLMSISE-00 empirical model (Picone et al., 2002), and compare its performance against the new TMDM. The complete assessment in this work includes, firstly, a statistical analysis of the different estimates during quiet and active magnetospheric activity on December 2015. Then, we include a dynamic orbit propagation of the 3 missions under different density input schemes and for different magnetospheric activity conditions, and 2-year statistical analysis of the differences to APOD (2016–2018) and Swarm-C (2014–2015) time-series.

The content in this manuscript is structured as follows: in the next section, a brief introduction of mass density estimates and space weather proxies employed in this work are introduced; Section 3 provides a summary of the data processing and analysis methods; results of data processing, interpretation of model deficiencies, and accuracy assessment are given in Section 4; finally, conclusions are summarized in the last section.

2. Data and models

2.1. The GRACE mission

GRACE was a joint mission between the National Aeronautics and Space Administration (NASA) and the Deutsches Zentrum Für Luft und Raumfahrt (DLR). The GRACE satellites were launched on March 17, 2002 to an initial altitude of approximately 500 km at a near-polar inclination of 89°, and with an orbital precession rate of about 322 days through 24 h of LST. GRACE measurements can be downloaded from the Information System and Data Center (ISDC) GeoForschungsZentrum (GFZ) website (http://isdc.gfz-potsdam.de/). The twin satellites of the GRACE mission were equipped with accurate accelerometers to measure the non-gravitational acceleration acting on the satellites, which can be used to derive atmospheric mass density estimates (Bruinsma et al., 2006; Sutton, 2008; Doornbos et al., 2010; Calabia and Jin, 2016, 2015).

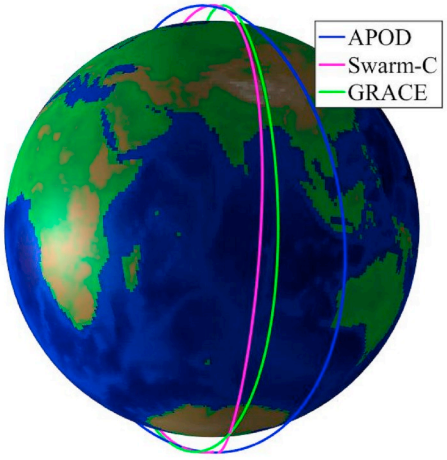

Fig. 1. One orbit cycle at 12 h UT, on December 20, 2015 for APOD, Swarm-C, and GRACE missions, showing the different locations along orbit paths. Orbits are plotted at 475 km altitude.

2.2. The Swarm mission

The Swarm satellites belong to the fifth Earth Explorer mission approved in ESA's (European Space Agency) Living Planet Programme, with a constellation of 3 identical satellites (A, B, and C) launched on November 22, 2013 into a near-polar orbit. SwarmA and Swarm-C are orbiting at an initial altitude of 462 km and at 87.35° inclination angle. Swarm-B is orbiting at an altitude of 511 km and at 87.75° inclination angle. The two lower satellites precess through 24 h of LST in 266 days, and the higher spacecraft in 288 days. Swarm measurements can be downloaded from the ESA website (ftp://Swarm-diss.eo.esa.int). Among other instruments, each Swarm satellite payload includes an accelerometer instrument to measure non-conservative forces, which can be used to derive atmospheric mass density estimates (Visser et al., 2013; Yuan et al. (2019)). In this study, we investigate Swarm-C orbit data and accelerometer-based mass density estimates.

2.3. The APOD mission

APOD is an initiative project operated by AFDL/BACC (Aerospace Flight Dynamics Laboratory/Beijing Aerospace Control Center) and launched on September 20, 2015, with 20 satellites successfully deployed into a near-polar circular orbit at 520 km altitude. Among these satellites, a set of 4 CubeSats conform the APOD mission, which is projected for atmospheric density estimation from in-situ measurements and precise orbit estimations. The lifetimes of these 4 CubeSats were set for 12 months, however, due to space weather conditions, the mission lifetime was extended for more than 2 years. Among other instruments, the APOD-A payload included an Atmospheric Density Detector (ADD) to investigate thermospheric mass density variability (Li et al., 2018; Tang et al., 2020). The other APOD-B/C/D satellites were too small to carry ADD instruments. After 2 weeks, the APOD-A descended to an altitude of 470 km and in-situ observations were taken for about 2 years. The ADD instrument was designed by the National Space Science Center (NSSC) of China. It was a space-borne sensor which performed in-situ temperature and pressure (p) estimates along orbit through voltage measurements (Li et al., 2018; Tang et al., 2020):

$$p = N_a \cdot m_2 \tag{1}$$

The term N_a is the atmosphere number density in terms of temperature and pressure observations (Clemmons et al., 2009; Tang et al., 2020; Li et al., 2018), and m_2 is the averaged molecular mass of the atmosphere. Since the APOD payload did not include a spectrometer for gas composition, the averaged molecular mass needs to be estimated, e.g., from the NRLMSIS-00 empirical model.

2.4. The NRLMSISE-00 model

The NRLMSISE-00 model is an empirical, global model of the Earth's atmosphere, from the ground to space, and is the standard for international space research. Primary use is to aid predictions of satellite orbital decay due to atmospheric drag.

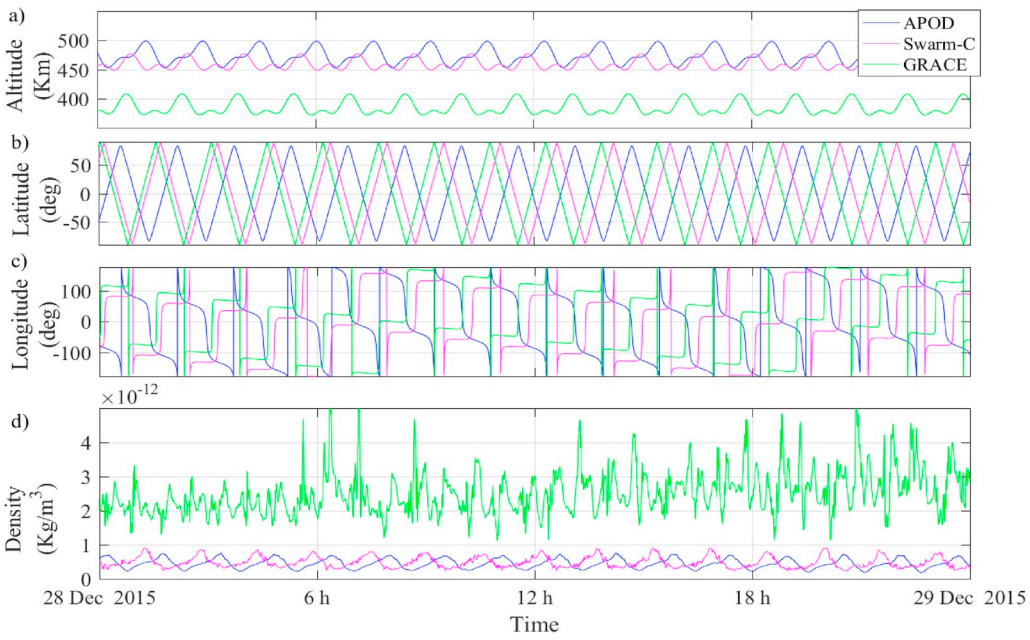

Fig. 2. The sparse nature of in-situ satellite observations during December 28, 2015, is shown along the orbital paths of APOD, Swarm-C, and GRACE satellites. From top to bottom, the panels show (a) altitudes, (b) latitudes, (c) longitudes, and (d) density estimates.

2.5. The TMDM model

The TMDM model is a new global empirical model of thermospheric mass density at LEO altitude, which is based on the fit of solar flux, annual, LST, and magnetospheric proxies using the PCA of 13 years of GRACE accelerometer-based mass density estimates. The base model employs the parameterizations provided in (Calabia and Jin (2016)) for the accurate characterization of thermospheric mass density under variable solar, annual, and LST cycles. The authors used the PCA to reduce 13 years time-series of GRACE mass density estimates into a low-dimensional space spanned by a set of modes. In brief, the aim of a PCA technique is to determine a new set of bases that capture the largest variance in the data, based on Eigen Value Decomposition of the covariance matrix. Detailed analyses and the selection of retained modes can be found in (Preisendorfer (1988) and Wilks (1995)), and a readily computable algorithm in (Bjornsson and Venegas, 1997). Recently, (Calabia and Jin, 2019) included to TMDM the fluctuations induced by magnetosphere forcing. The model can be downloaded from https://zenodo.org/record/3234582 , where the 4 leading modes together account for 99.8% of the total variance and, individually, explain 92%, 3.5%, 3%, and 1.3% of the total variability. The time-expansion PCA components were parameterized in terms of solar, annual, and LST cycles, and the space-expansion components in a set of spherical harmonic coefficients. The correlation coefficients between the parameterized time-expansion coefficients and the original coefficients are respectively 96%, 93%, 90%, and 83%. The high values of explained variance for the first modes indicate marked patterns of variability, and the correlations to the corresponding parameterizations indicate high accuracy in the model. In order to separately include the magnetosphere-forcing contribution through the parameterizations provided in Calabia and Jin, 2019, a constant value of 6 for the geomagnetic variation *Am* index need to be used in the base model.

2.6. Space weather and geomagnetic indices

Space weather and geomagnetic indices can be downloaded from the Low-Resolution OMNI (LRO) data set of NASA (http://omniweb.gsfc.nasa.gov/form/dx1.html), and from the International Service of Geomagnetic Indices (ISGI) website (http://isgi.unistra.fr/data_download.php).

3. Methodology

The accurate tracking and prediction of precise orbital ephemeris is the result of integrated knowledge of Earth's gravity field, upper atmosphere, and space weather conditions, where the trajectory of an orbiting object is propagated in a double integration and linearization of the Newton-Euler's equation of motion. The main forces involved in the dynamic POD include the variable gravity field, the atmospheric drag, and the solar (direct and reflected) and Earth's infrared radiation pressures (Montenbruck and Gill, 2013). In this work, we employ a simplified POD scheme were the Earth's infrared and the reflected solar radiation pressure are omitted due to their small magnitude (Jin et al., 2018). The drag acting on the satellite's surface is computed using the drag-force formula:

$$F_D = \frac{1}{2} CD \cdot A \cdot \rho \cdot v_r^2 \tag{2}$$

The term ***CD*** is the drag coefficient, ρ is the thermospheric mass density, A is the cross-sectional area perpendicular to the relative velocity of the atmosphere with respect to the spacecraft, which includes the co-rotating atmosphere and the horizontal winds (Jin et al., 2018). In this study, horizontal wind velocities have been omitted (see, Bruinsma et al., (2006)), and the velocity of the co-rotating atmosphere has been computed as the vector product between the Earth's angular rotation and the satellite's position vector. Under these equal assumptions for the three satellites employed in this work, the comparison in orbit propagation will provide a means to assess the different mass density inputs. We employ mass density estimates (ρ) along orbits to derive precise ephemeris of APOD, GRACE, and Swarm-C during December 18, 2015, when low magnetospheric activity was recorded (Ap = 3), and during the geomagnetic storm of December 21, 2015 (Ap = 111). Surface drag coefficients (*CD*) for each satellite are approximated values to Li et al., (2018), (Fig. 7) for APOD, March et al. (2019) (Fig. 12) for Swarm, and March et al. (2019) (Fig. 8) for GRACE. Cross-sectional areas (A) can be calculated from satellites' geometries given in Gu et al., (2017), Siemens (2018), and Bettadpur (2007), for APOD, Swarm and GRACE, respectively. Satellite mass for APOD is provided in Tang et al., 2020, and the masses for Swarm-C and GRACE are included in data-files of ESA and GFZ products, respectively. In this

scheme, by means of differences between precise GPS-based reduced-dynamic ephemeris and dynamically propagated ones, the resulting discrepancies will assess the effects produced by bias between models and in-situ estimates. We employ a dynamic POD propagator for the numerical solution of a differential-algebraic system of a first-order ordinary differential equation of the perturbed motion, based on variable-order implicit Runge-Kutta methods with a step-size control (Mahooti, 2009; Hairer and Wanner, 1996). The conservative force-model is recommended as for LEO satellites from Petit and Luzum (2010) up to degree 71. Their components include the EGM2008, the secular variations of its low-degree coefficients, the Moon and Sun third body tide, the solid Earth tides, the ocean tides, the solid Earth pole tide, the ocean pole tide, and the relativistic terms.

Usually, thermospheric mass densities (ρ) sampled at different altitudes are difficult to employ in different schemes and a re-scaling formula (Rentz and Lühr, 2008) can be defined as:

$$\rho^{h2} = \rho^{h1}_{obs} \frac{\rho^{h2}_{model}}{\rho^{h1}_{model}} \tag{3}$$

The term h1 is the original altitude and h2 is the required altitude. The errors caused by re-scaling are expected to be within 5% (Bruinsma et al., 2006). (Calabia and Jin (2016)) employed Equation (3) to re-scale GRACE mass densities to 475 km altitude, so the TMDM model could be extracted through the parameterizations of the main PCA modes. In this study we employ Equation (3) to re-scale the sparse nature of satellite density estimates to one common altitude for comparisons (from Figs. 2 to 3). In addition, the new TMDM model (which is given at 475 km) is re-scaled at the altitudes of APOD, Swarm, and GRACE density estimates for comparisons and POD computations.

4. Results

During December 2015, the APOD, Swarm-C, and GRACE satellites provided the unprecedented opportunity to compare simultaneous measurements (Fig. 1). Comparisons between model estimates (NRLMSISE-00 and TMDM) and in-situ estimates from APOD, Swarm-C, and GRACE during 20–21 and December 28, 2015 are shown in Figs. 3 and 4, where Equation (3) has been used to re-scale the values to 475 km along orbits. Fig. 2d shows the initial state of density values along orbits on December 28, 2015, with clear difficulties to compare the estimates if the re-scaling and a model re-sampling is not applied.

The different density states between Figs. 3 and 4 are caused by different magnetospheric conditions, where the Ap index for these periods correspond to Ap = 4 and Ap = 111, respectively. During the quiet conditions (Fig. 3), NRLMSISE-00 overestimates GRACE and Swarm-C estimates in about 1–2·10^{-13} kg/m^3, while APOD estimates seem to agree with similar values, although slightly out-of-phase by about 15 min. In the same conditions, TMDM shows good agreement with Swarm-C and GRACE estimates, while with APOD it overestimates along with NRLMSISE-00 in about 1–2·10^{-13} kg/m^3. Under the active magnetospheric conditions on 20–21 December 2015 (Fig. 4), NRLMSISE-00 and TMDM show good agreement, with some minor fluctuations. In this case, APOD and Swarm-C are overestimated compared to the models in the range ~10^{-12} kg/m^3, while GRACE agrees relatively well.

The differences for each mission (GRACE, Swarm-C, and APOD) on December 2015 are statistically investigated in Figs. 5–7 in terms of correlation, and relative error and standard deviation, with respect to background density. The results for GRACE show high correlation for quiet conditions (95%) going down to 75% during the geomagnetic storm of December 21, 2015. The mean of the error is zero and the standard deviation very low (1%), except for the period of high magnetospheric activity when the values rise up to 20%. Fig. 5 includes a comparison to NRLMSISE-00, where a clear overestimation by about 20% is clear in the mean error. The standard deviation to NRLMSISE-00 seems to be similar to that given by GRACE accelerometer estimates. The results for Swarm-C against TMDM (Fig. 6) show similar correlation, mean error, and standard deviation as for GRACE against TMDM. NRLMSISE-00 shows a clear overestimation over TMDM by about 40% in the mean error. The results for APOD against TMDM are considerably different (Fig. 7), showing a correlation of 80% and a mean error of 20%. The standard deviation is also higher than the previous Figures, showing values of about 25%. NRLMSISE-00 seems to have a lower difference in the mean error. The standard deviation is about 25%. Comparisons between NRLMSISE-00 and TMDM are included in these figures to assess the differences in each case. NRLMSISE-00 shows a mean overestimation of 20% with respect TMDM in the cases of GRACE and Swarm-C, and better correlation and lower standard deviation than observations in the APOD case (Fig. 7).

The assessment of models and observations in a dynamic orbit propagation scheme for two cases during this period is shown in Figs. 8–10. The left panels of Figs. 8–10 show the case studies on December 18, 2015, when low magnetospheric activity was recorded

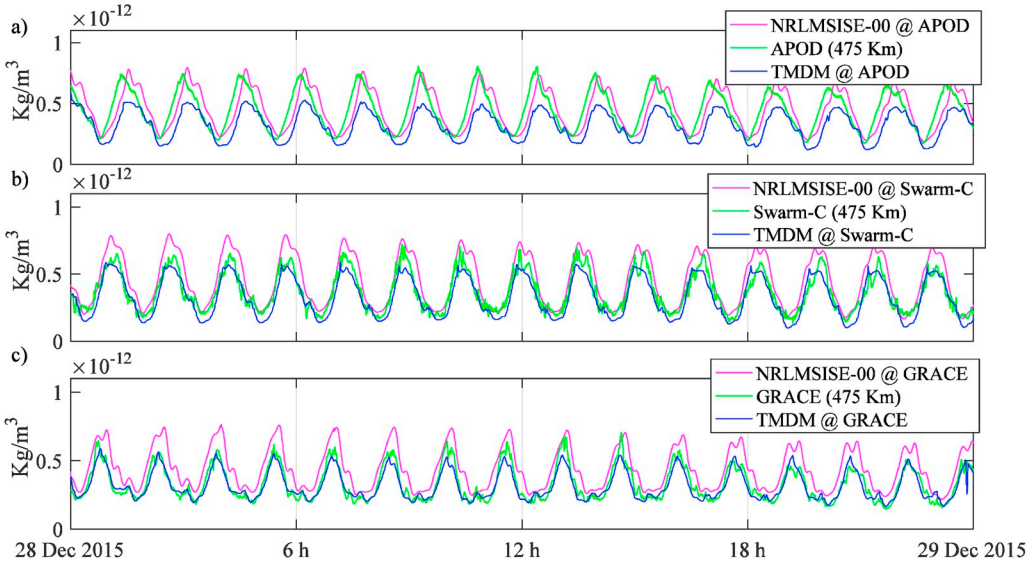

Fig. 3. Thermospheric mass density estimates from (a) APOD, (b) Swarm-C, and (c) GRACE, normalized to 475 km altitude (same as Fig. 2d but normalized to 475 km altitude). NRLMSISE-00 and TMDM are estimated at the same locations and times along the satellite orbits. During this period (28 December 2015) low magnetospheric activity was recorded (Ap = 4).

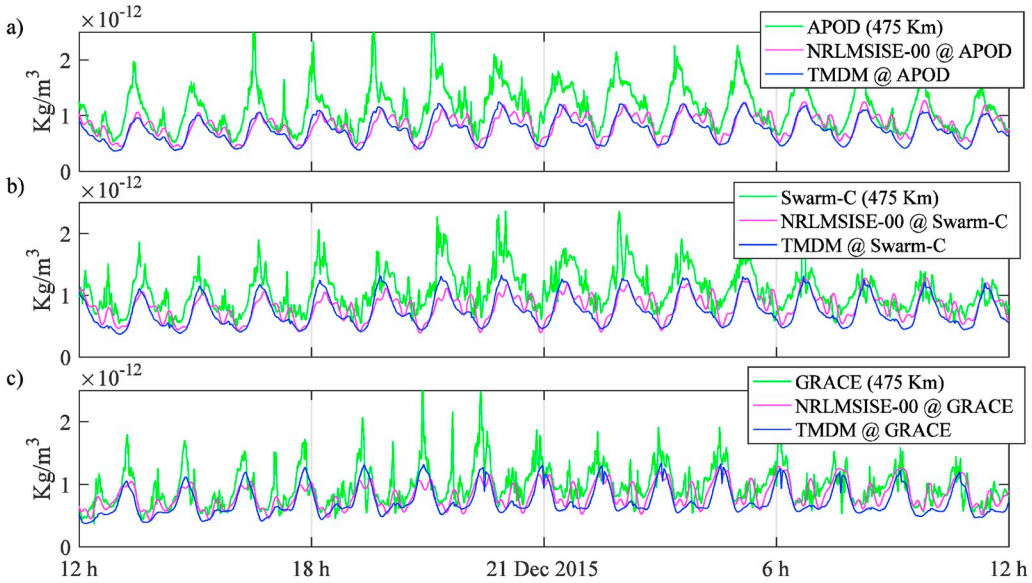

Fig. 4. Thermospheric mass density estimates from (a) APOD, (b) Swarm-C, and (c) GRACE, normalized to 475 km altitude. NRLMSISE-00 and TMDM are estimated at the same locations and times along the satellite orbits. Same plot as Fig. 3 but for the period of 20–21 December 2015, when high magnetospheric activity was recorded (Ap = 111).

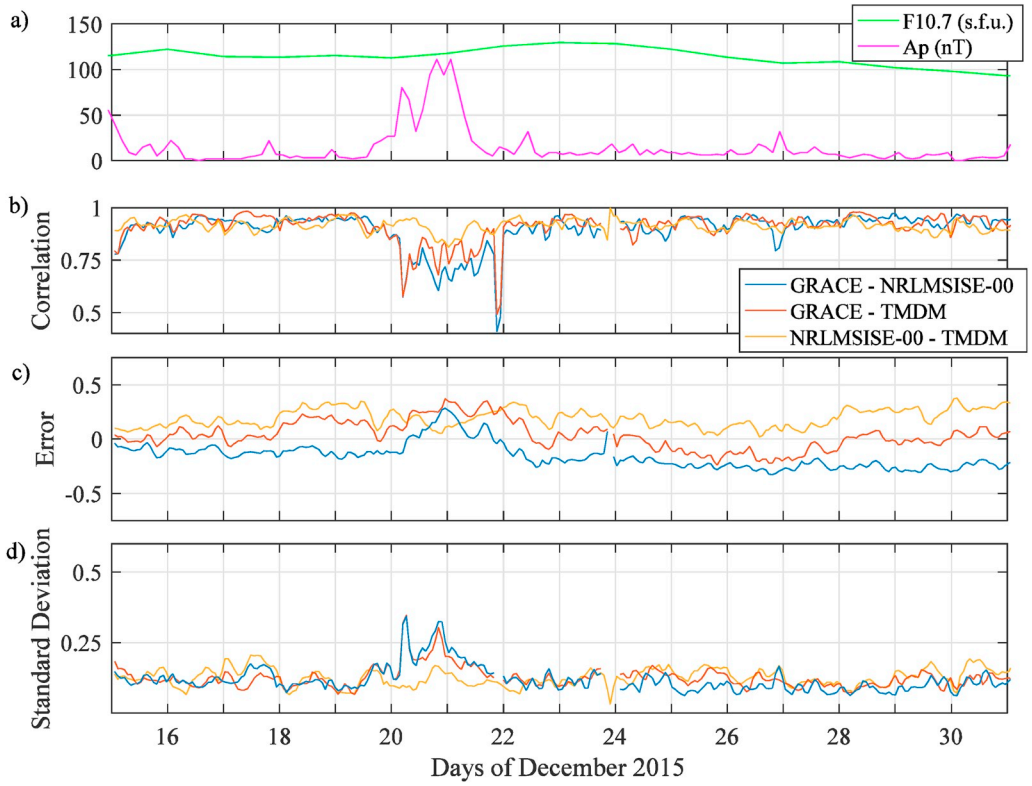

Fig. 5. Statistical analysis (dimensionless quantities) of residuals with respect to background density of GRACE estimates against TMDM and NRLMSISE-00 models for the last 15 days of December 2015 (data along GRACE orbit). Pearson's correlation is plotted in (b), the relative error (i.e., "[data1 – data2]/data2") is plotted in (c), and the standard deviation (i.e., "std{data1, data2}/data2") is plotted in (d). Solar flux (F10.7) and magnetospheric index (Ap) are show in the upper panel.

(Ap = 3), and the right panels on the same figures show the case studies during the geomagnetic storm (Ap = 111) on December 21, 2015. Mean altitudes during these periods for each mission can be seen in Fig. 2, where GRACE is located about 100 km below APOD and Swarm-C. Mass density estimates at the orbital height of APOD, GRACE and Swarm-C satellites inferred from ADD and accelerometer (ACC) instruments, and those estimated by TMDM and NRLMSISE-00 models show clearer similitude than that described in the previous paragraph. We plot the differences in the radial direction (dR) and the total position (dT) between the precise GPS-based reduced-dynamic POD ephemeris and the dynamically-propagated ephemeris in each scenario (true minus propagated). In each case, we employ the approximated drag-surface parameters presented in Table 1. Different values for drag parameters are presented in the literature (e.g., March et al., 2019), and these can

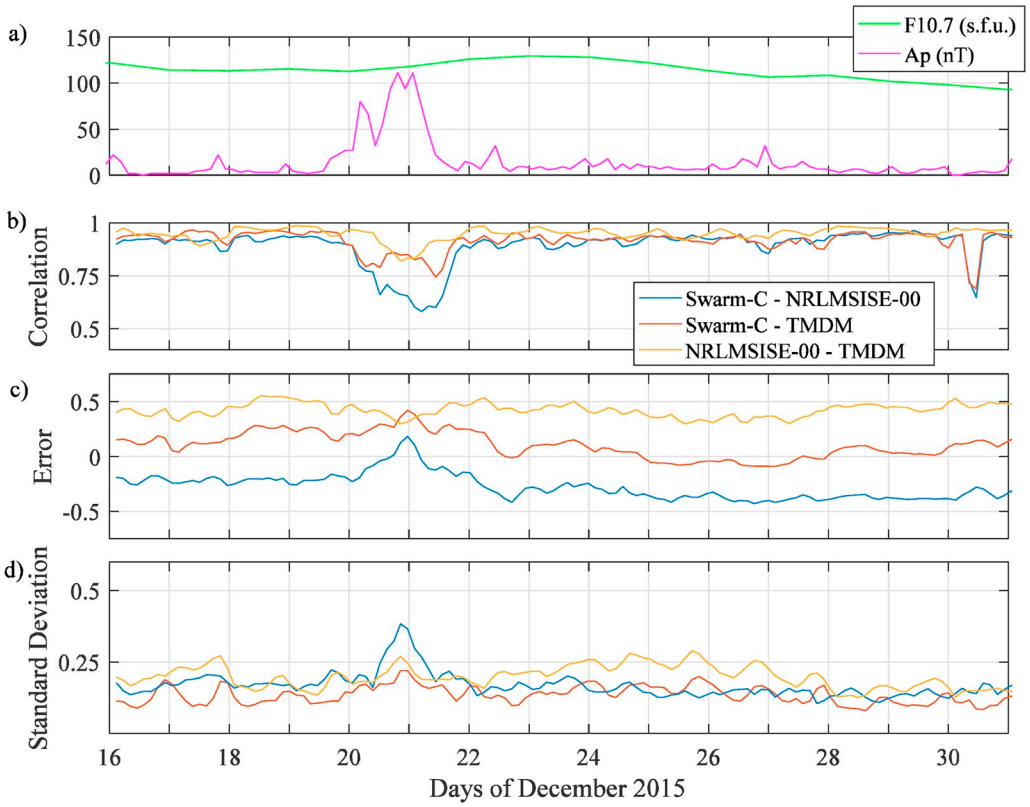

Fig. 6. Statistical analysis (dimensionless quantities) of residuals with respect to background density of Swarm-C estimates against TMDM and NRLMSISE-00 models for the last 15 days of December 2015 (data along Swarm-C orbit). Pearson's correlation is plotted in (b), the relative error (i.e., "[data1 – data2]/data2") is plotted in (c), and the standard deviation (i.e., "std{data1, data2}/data2") is plotted in (d). Solar flux (F10.7) and magnetospheric index (Ap) are show in the upper panel.

provide very different results in the propagated orbits. In fact, actual orbit errors could be provided if reliable density estimates and drag coefficients were employed, but the difficulties related to drag-force modeling are still in development and the 'actual' mass density of the variable thermosphere is still unknown. Note that thermospheric mass density derived from satellite drag coefficient (Equation (2)) depends on many factors, including energy accommodation, gas-surface interaction, molecular reflections distribution, atmospheric compositions and temperature, and satellite geometry, speed, attitude, temperature, composition, etc. Among these, energy accommodation, molecular reflections distribution, and gas-surface interaction are critical parameters for deriving mass densities (Mehta et al., 2014), but the current difficulties for estimation and lack of direct measurements increase the uncertainty of thermospheric mass density estimation from satellite drag. For this reason, this analysis might merely aim to show the "discrepancies" between different schemes of density input, and not the "actual errors" derived from deviation to the actual background density.

In panels (b) and (e) of Figs. 8–10, positive/negative values in the radial direction (dR) indicate an overestimation/underestimation of mass density state for the adopted surface-drag parameters (Table 1). In general, the total differences in position (dT) show smaller values during quiet time (c) than during the geomagnetic storm (f), and are less pronounced at the lower altitudes of GRACE (Fig. 10). During quiet conditions (left panels), the differences between TMDM and in-situ observations after 6 h remain under 50 m, while during active conditions (right panels) these can reach up to 100 m. In general, the new TMDM performs under different magnetospheric conditions within a similar error range to that given by NRLMSISE-00. Differences between both models are less than 50 m after 6 h.

The long term statistical analyses of differences between Swarm-C and APOD are shown in Figs. 11 and 12. The Swarm-C mission provided estimates from February 2014 to June 2016, while APOD from December 2015 to January 2018. The correlation coefficients show higher agreement between models to Swarm-C (~90%) while APOD correlates at about 80%. Interesting reductions down to 50% in correlation is shown in Swarm-C during June, October 2014, and March, August December, and April 2016, which might be related to the LST cycle (Fig. 11b). The mean error in both cases shows similar behavior, overestimating TMDM in 20% and underestimating NRLMSISE-00 in −20% the background density, though NRLMSISE-00 shows some fluctuations along with the time series. The standard deviation shows a mean value of 10% for Swarm-C (Figs. 11d) and 20% for APOD (Fig. 12d), fluctuating for the last one from an unknown source.

5. Conclusions

This paper has shown the assessment of the new TMDM model by GRACE, APOD, Swarm-C and NRLMSISE-00 estimates under different schemes. Comparisons on December 2015 show good agreement between TMDM and Swarm-C, while APOD and NRLMSISE-00 seem to overestimate by about 20% the background state. The correlation between Swarm-C and TMDM has shown a mean value of 95%, and the standard deviation of differences about 1% (with respect to the background density). Estimates from the ADD instrumentation (APOD) have shown lower values of correlation (80%), and higher standard deviation (25%). We have investigated the dynamic orbit propagation under different conditions and compared the results to GPS-based precise orbit ephemeris, for low magnetospheric activity on December 18, 2015 (Ap = 3), and for the geomagnetic storm of December 21, 2015 (Ap = 111). All cases have shown similar discrepancies in orbit propagation after 6 h, showing values up to 50–100 m depending on magnetospheric conditions. In comparison with NRLMSISE-00, the new TMDM performs better than we expected, showing good response under different magnetospheric conditions. We consider TMDM as a good candidate to

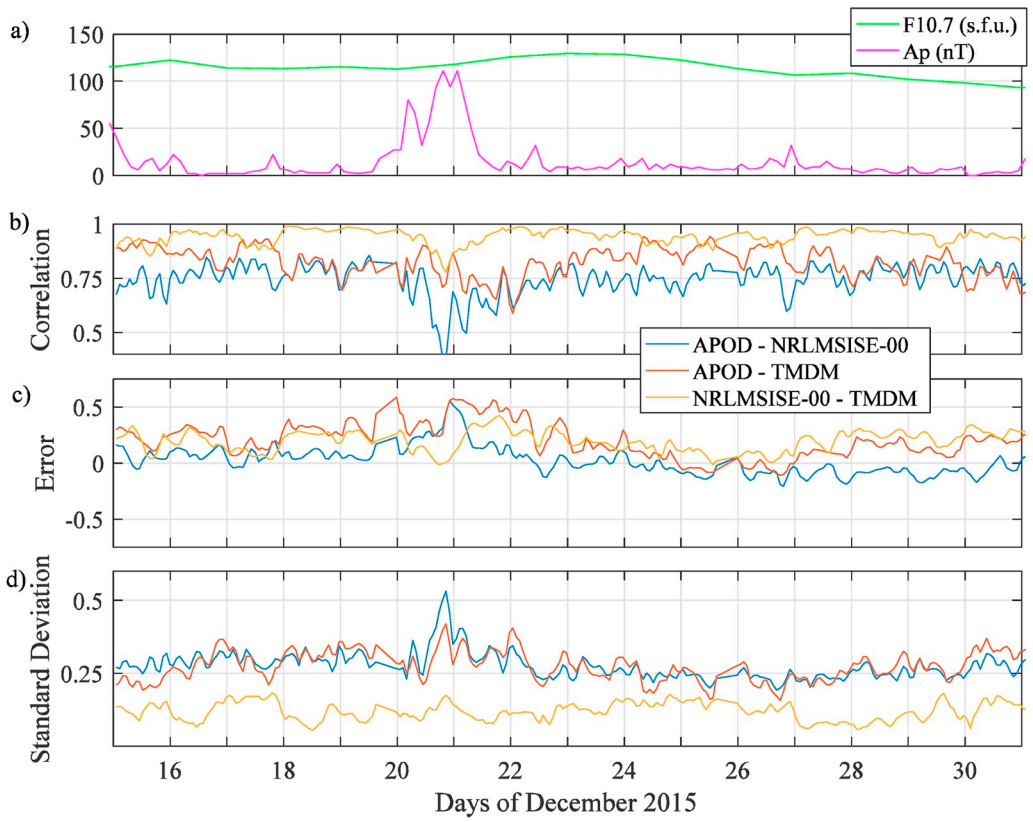

Fig. 7. Statistical analysis (dimensionless quantities) of residuals with respect to background density of APOD estimates against TMDM and NRLMSISE-00 models for the last 15 days of December 2015 (data along APOD orbit). Pearson's correlation is plotted in (b), the relative error (i.e., "[data1 – data2]/data2") is plotted in (c), and the standard deviation (i.e., "std{data1, data2}/data2") is plotted in (d). Solar flux (F10.7) and magnetospheric index (Ap) are show in the upper panel.

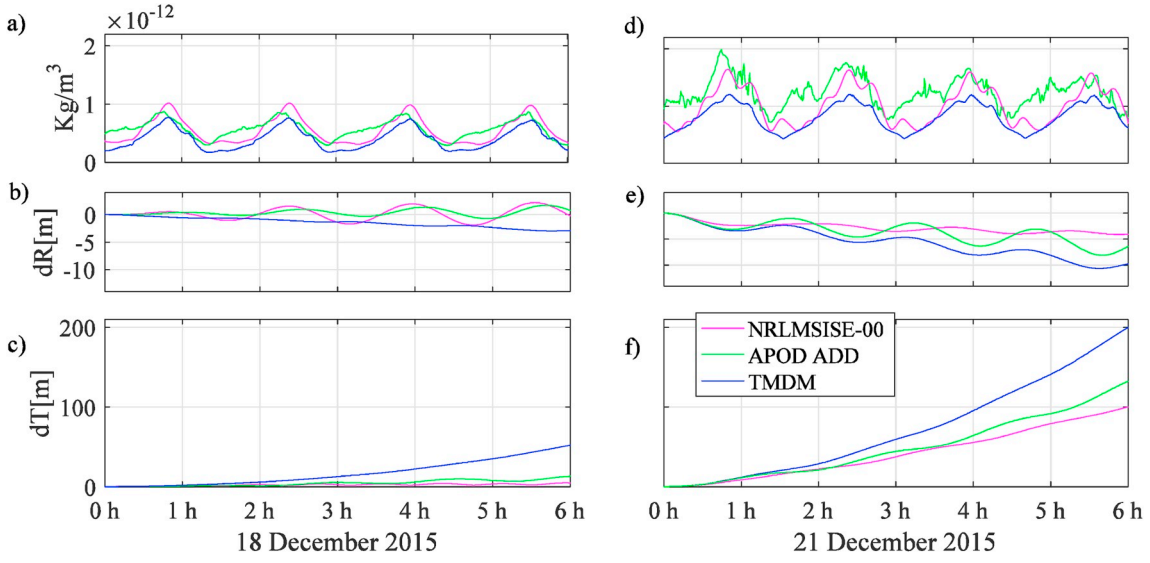

Fig. 8. Top panels (a, d) show thermospheric mass densities at orbital height for APOD satellite path inferred from ADD instrument, and those estimated by TMDM and NRLMSISE-00 model. Middle panels (b, e) and bottom panels (c, f) show the differences in radial (dR) and total (dT) position between the precise GPS-based reduced-dynamic POD ephemeris and the dynamically-propagated ephemeris in each scenario (true-propagated). Left panels for December 18, 2015 (Ap = 3) and right panels for December 21, 2015 (Ap = 111).

be used as an example for future research and modeling.

The statistical analysis of differences along 2 years of Swarm-C (2014–2016) and APOD (2016–2018) against NRLMSISE-00 and TMDM show correlations over 90% for Swarm-C and about 80% for ADD instrumentation (APOD). The mean values of differences along Swarm-C show a bias of about 20% with respect TMDM and about −20% with respect NRLMSISE-00, while the standard deviations for both cases show about 10% of the background density. The mean values of differences along APOD show a bias of about 20% with respect TMDM and −20% with respect NRLMSISE-00, while the standard deviations for both cases

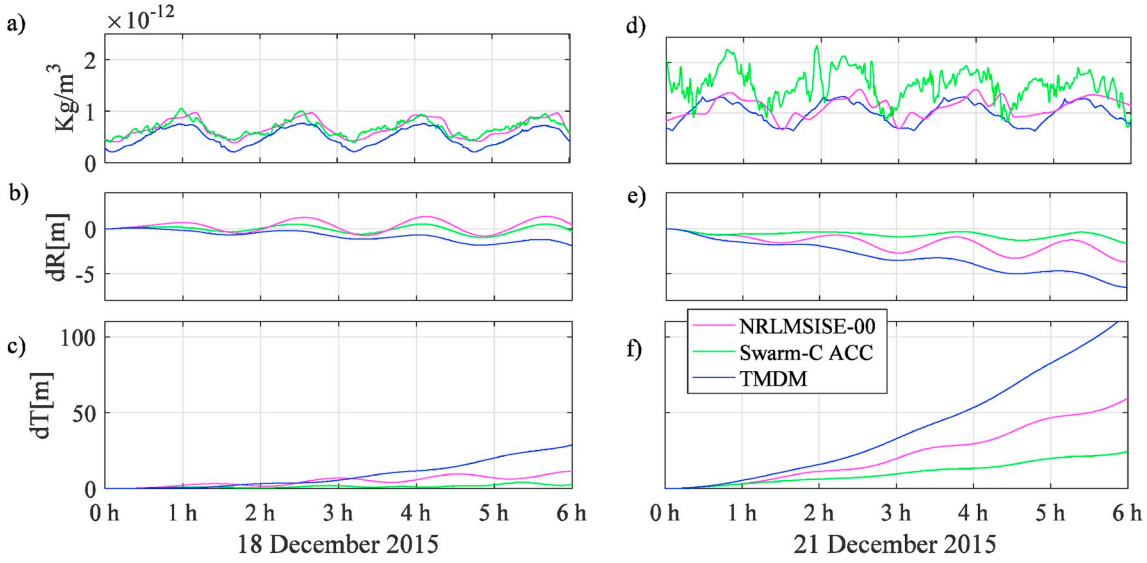

Fig. 9. Top panels (a, d) show thermospheric mass densities at orbital height for Swarm-C satellite path inferred from accelerometer, and those estimated by TMDM and NRLMSISE-00 model. Middle panels (b, e) and bottom panels (c, f) show the differences in radial (dR) and total (dT) position between the precise GPS-based reduced-dynamic POD ephemeris and the dynamically-propagated ephemeris in each scenario (true-propagated). Left panels for December 18, 2015 (Ap = 3) and right panels for December 21, 2015 (Ap = 111).

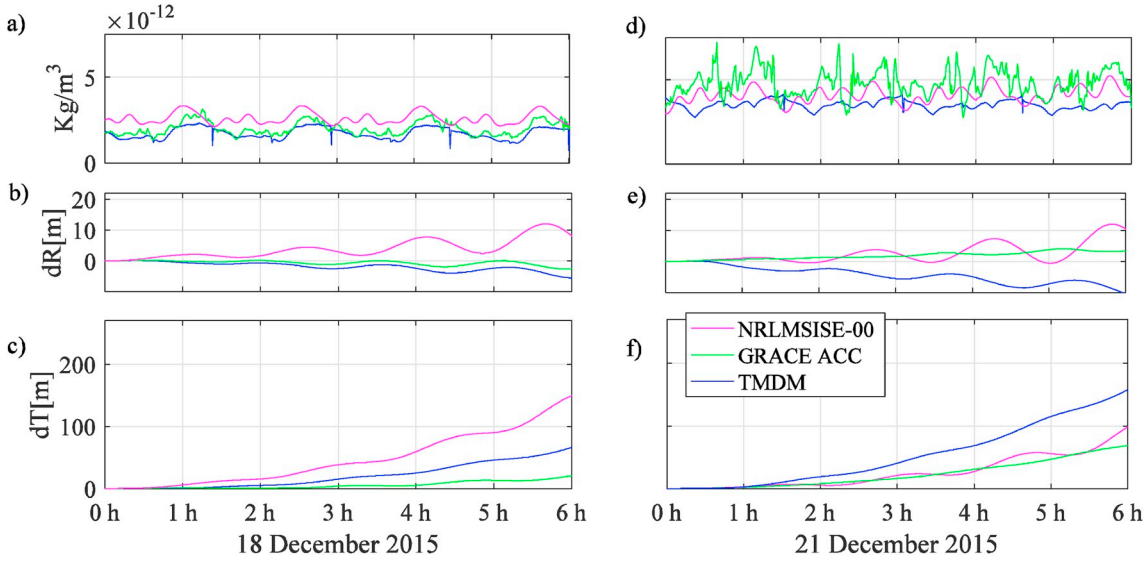

Fig. 10. Top panels (a, d) show thermospheric mass densities at orbital height for GRACE satellite path inferred from accelerometer, and those estimated by TMDM and NRLMSISE-00 model. Middle panels (b, e) and bottom panels (c, f) show the differences in radial (dR) and total (dT) position between the precise GPS-based reduced-dynamic POD ephemeris and the dynamically-propagated ephemeris in each scenario (true-propagated). Left panels for December 18, 2015 (Ap = 3) and right panels for December 21, 2015 (Ap = 111).

Table 1
Surface parameters and mass employed in the dynamic orbit propagation.

	APOD	Swarm-C	GRACE
Effective area for drag (m^2)	0.153	1.0	1.21
Drag coeff. (CD)	3.0	3.4	3.4
Effective area for solar radiation (m^2)	0.154	7.5	6
Radiation coeff. (CR)	1	1.2	1.2
Satellite mass for Dec. 2015 (kg)	25.88	433	461.5

are about 20% of the background density.

These deviations with respect to NRLMSISE-00 and TMDM might suggest that additional recalibration of models and revisions of algorithms are required to derive mass density estimates from in-situ measurements. For example, a scaling factor of 0.8 multiplied to NRLMSISE-00, and 1.2 multiplied to TMDM. However, using the averaged molecular mass density from NRLMSISE-00 (Equation (1)) and the difficulties related to drag-force modeling still introduce unexpected biases in ADD and ACC estimates, respectively, as shown in this work. As shown in the literature (e.g., Mehta et al., 2014; March et al., 2019), it is clear whether more research is required to estimate or directly measure accurate drag coefficients of different satellites. Key parameters including energy accommodation, molecular reflections distribution, and gas-surface interaction, have potential to provide high accuracy when deriving thermospheric mass densities from satellite drag.

Monitoring and modeling Earth's upper atmosphere processes is a key fundamental to better understand how space weather responds to variable solar and magnetospheric conditions and to forecast the

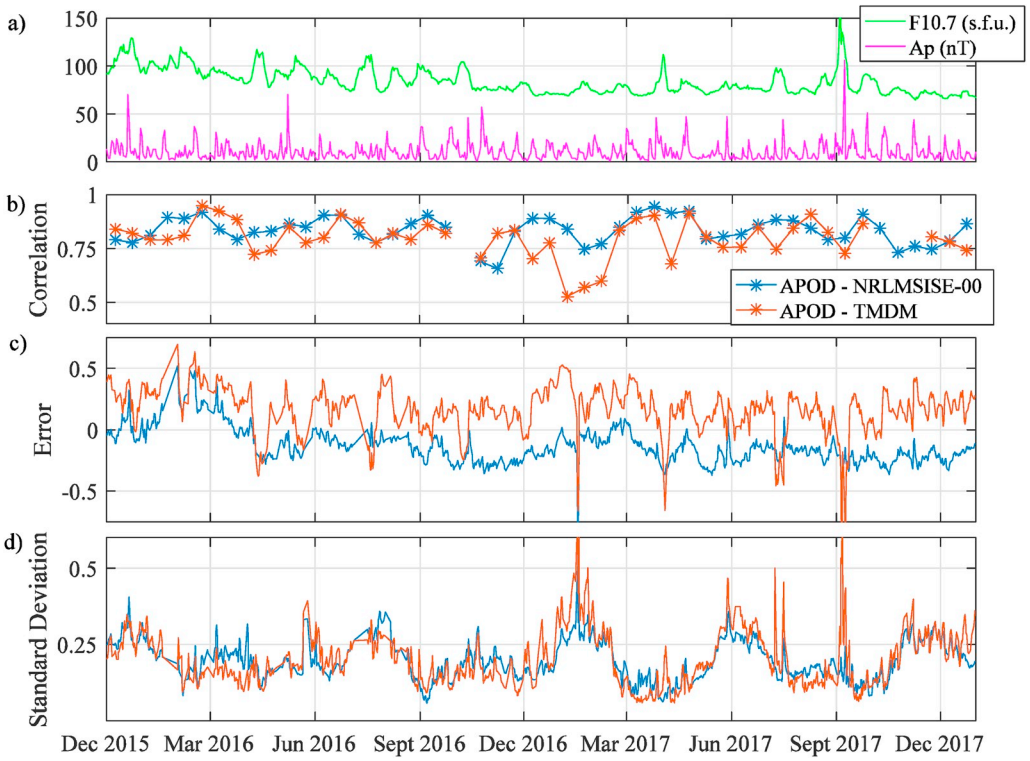

Fig. 11. Statistical analysis (dimensionless quantities) of residuals with respect to background density of APOD estimates against TMDM and NRLMSISE-00 models for the period December 2015 to January 2018 (data along APOD orbit). Pearson's correlation is plotted in (b), the relative error (i.e., "[data1 – data2]/data2") is plotted in (c), and the standard deviation (i.e., "std{data1, data2}/data2") is plotted in (d). Solar flux (F10.7) and magnetospheric index (Ap) are show in the upper panel.

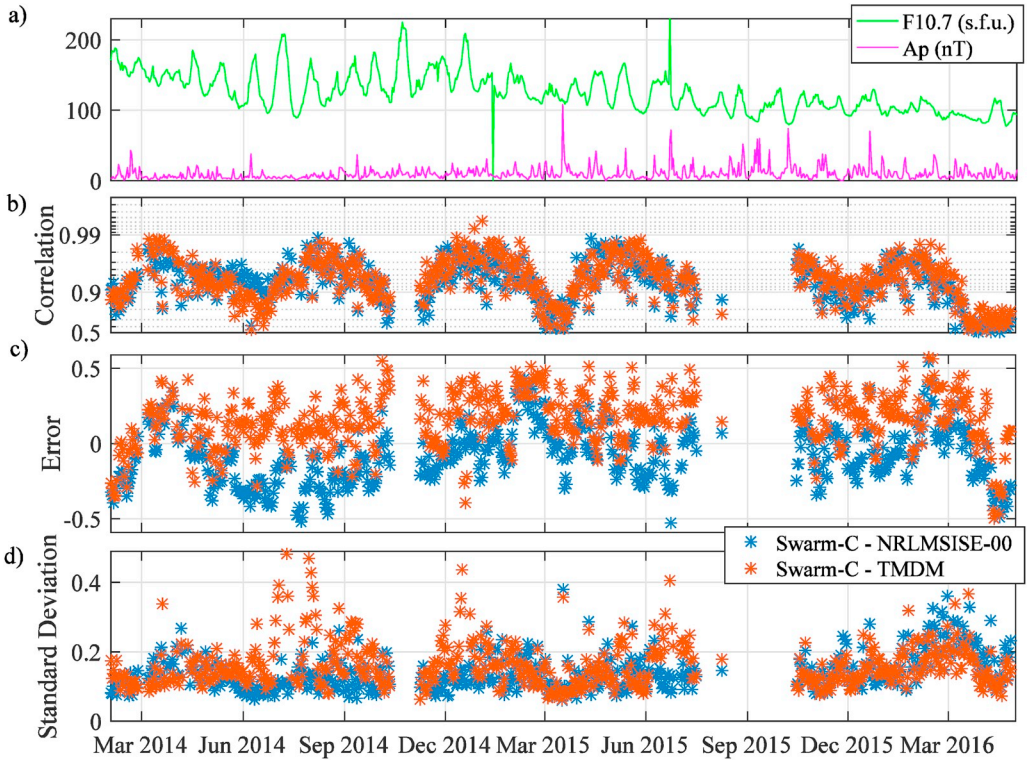

Fig. 12. Statistical analysis (dimensionless quantities) of residuals with respect to background density of Swarm-C estimates against TMDM and NRLMSISE-00 models for the period February 2014 to June 2016 (data along APOD orbit). Pearson's correlation is plotted in (b), the relative error (i.e., "[data1 – data2]/data2") is plotted in (c), and the standard deviation (i.e., "std{data1, data2}/data2") is plotted in (d). Solar flux (F10.7) and magnetospheric index (Ap) are show in the upper panel.

detrimental effects on life and society. For instance, increases in solar activity produce an augment of mass density in the upper atmosphere, and the resulting increase of drag force on LEO objects causes uncontrolled orbital decay and reentry. Unfortunately, the negative effects of miss-modeled variations in aerodynamic drag results in positioning errors far to meet the operational requirements in orbital tracking, and the negative repercussions and concerns in the space industry and space situational awareness force to demand better modeling of the upper atmospheric mass density distribution and variations. Therefore, new models, estimates, and differences between them can help to better understand the complex processes in the Ionosphere-Thermosphere system by calibrating physics-based models.

Acknowledgments

This work was supported by the National Natural Science Foundation of China-German Science Foundation (NSFC-DFG) Project (Grant No. 41761134092), the Startup Foundation for Introducing Talent of NUIST (Grant No. 2243141801036), and the Talent Start-Up Funding projects of NUIST (Grant No. 1411041901010 and Grant No. 2241041801074). Great appreciation is extended to ISDC, ESA, NASA, and AFDL/BACC for providing the data access. There is no conflict of interest regarding the publication of this paper.

References

Anderson, R.L., George, H.B., Forbes, J.M., 2009. Sensitivity of orbit predictions to density variability. J. Spacecraft Rockets 46 (6), 1214–1230. https://doi.org/10.2514/1.42138.

Bettadpur, S., 2007. Gravity Recovery and Climate Experiment Product Specification Document (Rev 4.5 – February 20, 2007). Tech. Rep., GRACE 327-720/CSR-GR-03-02. Center for Space Research, The University of Texas at Austin.

Bjornsson, H., Venegas, S.A., 1997. A Manual for EOF and SVD Analyses of Climatic Data. McGill Univ., Montréal, Québec, p. 52. CCGCR Report No. 97-1.

Bruinsma, S., Forbes, J.M., Nerem, R.S., Zhang, X., 2006. Thermosphere density response to the 20–21 November 2003 solar and geomagnetic storm from CHAMP and GRACE accelerometer data. J. Geophys. Res. 111, A06303. https://doi.org/10.1029/2005JA011284.

Calabia, A., Jin, S.G., 2015. GPS-based non-gravitational accelerations and accelerometer calibration. In: Jin, S. (Ed.), Satellite Positioning: Methods, Models and Applications. InTech-Publisher, Rijeka, Croatia, pp. 47–72.

Calabia, A., Jin, S.G., 2016. New modes and mechanisms of thermospheric mass density variations from GRACE accelerometers. J. Geophys. Res. Space Phys. 121 (11), 11191–11212. https://doi.org/10.1002/2016JA022594.

Calabia, A., Jin, S.G., 2019. Solar cycle, seasonal, and asymmetric dependencies of thermospheric mass density disturbances due to magnetospheric forcing. Ann. Geophys. 37 (5), 989–1003. https://doi.org/10.5194/angeo-37-989-2019.

Clemmons, J.H., Friesen, L.M., Katz, N., et al., 2009. The ionization Gauge investigation for the Streak mission. Space Sci. Rev. 145 (200), 263–283. https://doi.org/10.1007/s11214-009-9489-6.

Doornbos, E., J Van Den IJssel, H.L., Forster, M., Koppenwallner, G., 2010. Neutral density and crosswind determination from arbitrarily oriented multiaxis accelerometers on satellites. J. Spacecraft Rockets 47 (4), 580–589. https://doi.org/10.2514/1.48114.

Emmert, J.T., 2015. Thermospheric mass density: a review. Adv. Space Res. 56 (5), 773–824. https://doi.org/10.1016/j.asr.2015.05.038.

Gu, D., Liu, Y., Yi, B., Cao, J., Li, X., 2017. In-flight performance analysis of MEMS GPS receiver and its application to precise orbit determination of APOD-A satellite. Adv. Space Res. 60 (12) https://doi.org/10.1016/j.asr.2017.08.023.

Hairer, A., Wanner, G., 1996. Solving ordinary differential equations II. In: Stiff and Differential-Algebraic Problems. Springer Series in Computational Mathematics, vol. 14. Springer-Verlag Berlin Heidelberg, 1991.

Jin, S.G., Calabia, A., Yuan, L.L., 2018. Thermospheric variations from GNSS and accelerometer measurements on small satellites. Proc. IEEE 103 (3), 484–495. https://doi.org/10.1109/JPROC.2018.2796084.

Leonard, J.M., Forbes, J.M., Born, G.H., 2012. Impact of tidal density variability on orbital and reentry predictions. Space Weather 10 (12), 12003. https://doi.org/10.1029/2012SW000842.

Li, X., Xu, J.Y., Tang, G.S., et al., 2018. Processing and calibrating of in-situ atmospheric densities for APOD. Chin. J. Geophys. 61 (9), 3567–3576. https://doi.org/10.6038/cjg2018L0452 (in Chinese).

Mahooti, M., 2009. *Orbit Propagation of LEO Satellites Applying Multi-Step and Single-step Integrators*, EGU General Assembly Conference Abstracts, vol. 11. Arabelos, D.N. and Tscherning, C.C., p. 6749

March, G., Doornbos, E.N., Visser, P.N.A.M., 2019. High-fidelity geometry models for improving the consistency of CHAMP, GRACE, GOCE and Swarm thermospheric density data sets. Adv. Space Res. 63 (1), 213–238. https://doi.org/10.1016/j.asr.2018.07.009.

March, G., Visser, T., Visser, P.N.A.M., Doornbos, E.N., 2019. CHAMP and GOCE thermospheric wind characterization with improved gas-surface interactions modelling. Adv. Space Res. 64 (6), 1225–1242. https://doi.org/10.1016/j.asr.2019.06.023.

Mehta, P.M., Walker, A., McLaughlin, C.A., Koller, J., 2014. Comparing physical drag coefficients computed using different gas–surface interaction models. J. Spacecraft Rockets 51–3, 873–883. https://doi.org/10.2514/1.A32566.

Montenbruck, O., Gill, E., 2013. Satellite Orbits: Models, Methods and Applications. Springer, Berlin.

Petit, G., Luzum, B., 2010. IERS conventions (2010). In: IERS Tech. Note, vol. 36. Verlag des Bundesamts für Kartogr. und Geod, Frankfurt am.

Picone, J.M., Hedin, A.E., Drob, D.P., Aikin, A.C., 2002. NRLMSISE-00 empirical model of the atmosphere: statistical comparisons and scientific issues. J. Geophys. Res. 107 (A12), 1468. https://doi.org/10.1029/2002JA009430.

Preisendorfer, R., 1988. Principal Component Analysis in Meteorology and Oceanography. Elsevier, Amsterdam.

Rentz, S., Lühr, H., 2008. Climatology of the cusp-related thermospheric mass density anomaly, as derived from CHAMP observations. Ann. Geophys. 26, 2807–2823. https://doi.org/10.5194/angeo-26-2807-2008.

Siemes, C., 2018. Swarm Satellite Thermo-Optical Properties and External Geometry. ESA-EOPG-MOM-MO-15. Tech. rep., ESA.

Sutton, E.K., 2008. Effects of Solar Disturbances on the Thermosphere Densities and Winds from CHAMP and GRACE Satellite Accelerometer Data. Thesis. Department of aerospace engineering sciences.

Tang, G., Li, X., Cao, J., Liu, S., Chen, G., Man, H., Zhang, X., Shi, S., Sun, J., Li, Y., Calabia, A., 2020. APOD mission status and preliminary results. Sci. China Earth Sci. 63, 257–266. https://doi.org/10.1007/s11430-018-9362-6.

Visser, P., Doornbos, E., van den IJssel, J., Teixeira da Encarnação, J., 2013. Thermospheric density and wind retrieval from Swarm observations. Earth Planets Space 65 (11), 1319–1331. https://doi.org/10.5047/eps.2013.08.003.

Wilks, D.S., 1995. Statistical Methods in the Atmospheric Sciences. Academic Press, San Diego, Calif.

Yuan, L.L., Jin, S.G., Calabia, A., 2019. Distinct thermospheric mass density variations following the September 2017 geomagnetic storm from GRACE and Swarm. J. Atmos. Sol. Terr. Phys. 184, 30–36. https://doi.org/10.1016/j.jastp.2019.01.007.